

Journal Pre-proof

Curing kinetics of dually-processed acrylate-epoxy 3D printing resins

Osman Konuray, José M. Morancho, Xavier Fernández-Francos,
Montserrat García-Alvarez, Xavier Ramis



PII: S0040-6031(21)00104-0
DOI: <https://doi.org/10.1016/j.tca.2021.178963>
Reference: TCA 178963

To appear in: *Thermochimica Acta*

Received Date: 24 March 2021
Revised Date: 11 May 2021
Accepted Date: 12 May 2021

Please cite this article as: Konuray O, Morancho JM, Fernández-Francos X, García-Alvarez M, Ramis X, Curing kinetics of dually-processed acrylate-epoxy 3D printing resins, *Thermochimica Acta* (2021), doi: <https://doi.org/10.1016/j.tca.2021.178963>

This is a PDF file of an article that has undergone enhancements after acceptance, such as the addition of a cover page and metadata, and formatting for readability, but it is not yet the definitive version of record. This version will undergo additional copyediting, typesetting and review before it is published in its final form, but we are providing this version to give early visibility of the article. Please note that, during the production process, errors may be discovered which could affect the content, and all legal disclaimers that apply to the journal pertain.

© 2020 Published by Elsevier.

Curing kinetics of dually-processed acrylate-epoxy 3D printing resins

Osman Konuray¹, José M. Morancho¹, Xavier Fernández-Francos¹, Montserrat García-Alvarez², Xavier Ramis^{1*}

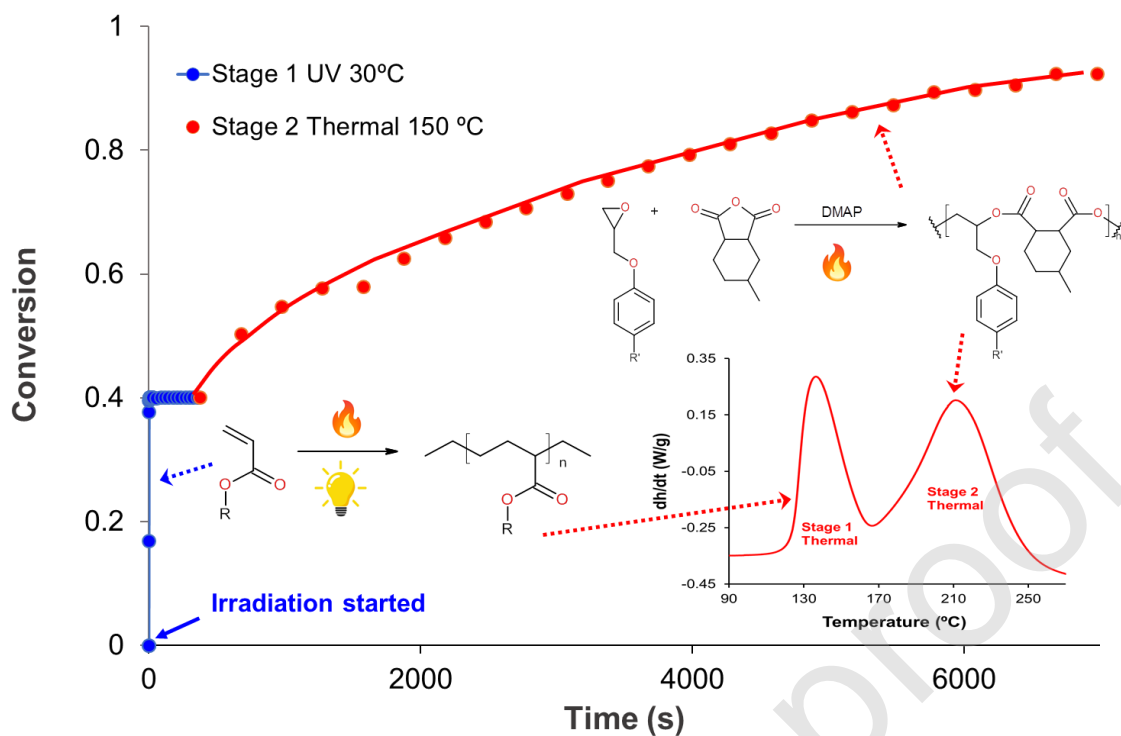
¹ Thermodynamics Laboratory, ETSEIB Universitat Politècnica de Catalunya, Av. Diagonal 647, 08028, Barcelona, Spain

² Department of Chemical Engineering, ETSEIB Universitat Politècnica de Catalunya, Av. Diagonal 647, 08028, Barcelona, Spain

*Corresponding author: Tel.: +34 934016592; fax: + 34 934017389

E-mail address: xavier.ramis@upc.edu

Graphical Abstract



Highlights

- Photo/thermal dual-curing of a ternary acrylate-epoxy-anhydride mixture is studied.
- Acrylate photopolymerization is followed by thermal epoxy-anhydride copolymerization.
- Isoconversional dynamic kinetic parameters can be used to simulate isothermal curing.
- The isokinetic relationship proved to be a powerful tool to analyze dual-curing kinetic.

Abstract

In this work, the curing kinetics of a new ternary acrylate/epoxy/anhydride thermoset system which is used for dual-curing 3D-printing applications is studied. The first curing stage is an acrylate free-radical photopolymerization that can also be triggered using a suitable thermal radical initiator. The second curing stage is an epoxy-anhydride copolymerization initiated at higher temperatures by a nucleophilic tertiary amine. Isothermal acrylate photocure kinetics was modeled using a first order rate expression. The thermal curing of both reaction stages was studied under by non-isothermal integral isoconversional and model fitting methods. Furthermore, they were successfully reproduced using a simulation based on the obtained kinetic parameters. Reduced master curves and isokinetic relationships were used to validate the kinetic model selected and the reliability of the employed methodology. The conditions for obtaining a thermal and sequential dual curing can be established with the help of isokinetic temperature.

Keywords

Kinetics, Acrylate; epoxy; dual-curing; 3D-printing

1 Introduction

Freedom of design, mass customization, waste minimization and the ability to manufacture complex structures, as well as fast prototyping, are the main benefits of additive manufacturing (AM) or 3D printing [1-3]. Stereolithography (SL) and digital light processing (DLP) of acrylate based-formulations are commonly used techniques in the 3D-printing of thermosetting polymer parts. SL and DLP are based on layer-by-layer solidification of liquid-like reactive thermosetting formulations upon exposure to UV or visible light. SL and DLP processing lead to crosslinked materials with superior properties and higher resolutions in comparison with other AM techniques. However, SL and DLP techniques face certain challenges, in particular regarding material properties such as mechanical anisotropy, porosity, geometrical accuracy, and appearance [4,5].

Hybrid dual-cure formulations combining UV radical homopolymerization of acrylates at room temperature with epoxy-curing at higher temperatures are recognized to enhance the quality of printed parts significantly. This is due to reduced shape distortion during cure and also to the further post-cure after printing. The latter increases the overall degree of curing and reduces inhomogeneity. Recently, cationic cycloaliphatic epoxy homopolymerization and epoxy/anhydride or epoxy/dicyandiamide copolymerization, have been successfully used as a secondary, thermal curing stage, following acrylate photopolymerization. Homogenous and fully cured materials with improved mechanical properties have generally been obtained [4-10]. Significant improvements have also been achieved by adding a radical thermal initiator, that can be activated during the second curing stage [5,7-10]. The addition of thermal initiators and a careful selection of curing temperatures enables the sequential dual-curing of these materials under thermal activation, if desired [8,9].

Recently, our group described a new hybrid system consisting of a commercial 3D printing acrylate resin modified by an epoxy-anhydride mixture that imparts rigidity to the final materials [11]. Final materials showed properties far superior to those of the commercial resin and excellent shape memory capability was documented as well. Moreover, large objects could be manufactured by printing them in halves, followed by joining the halves permanently at the second cure stage. As these materials showed good potential of applicability, in this work, their dual-curing kinetics will be studied in depth.

In general, the knowledge of the curing kinetics of thermosets is a fundamental tool for their successful processing. With a few and quick experiments, it is possible to know, at least tentatively, the adequate processing times and temperatures, even out of the experimental range of the tests. This is especially important in dual-curable formulations with several reagents and initiators whose interactions can lead to complex kinetic effects. Well established curing kinetics allow control over curing sequence and storage stability in one-pot dual-curable formulations.

Photocuring is always performed under isothermal conditions, due to the low curing time of acrylates and due to the fact that kinetics hardly depend on temperature. However, for thermally controlled curing, there are many approaches, each with its own advantages and disadvantages and degree of reliability. An excellent discussion is provided in the work of Vyazovkin *et al.* [12].

The first curing stage of our acrylate/epoxy/anhydride ternary system is a radical photopolymerization of acrylate groups, which was studied isothermally at 30 °C using a phenomenological n^{th} order model. The second stage is an epoxy-anhydride copolymerization catalyzed by 4-(dimethylamino)pyridine as anionic initiator. As mentioned, it is possible to carry out the first stage purely thermally by using 1,1-di(*t*-amylperoxy)-cyclohexane, a thermal radical initiator. Both thermal reactions were

studied using integral isoconversional dynamic procedure and autocatalytic model fitting. The so-called kinetic triplet, which consists of the activation energy, pre-exponential factor and conversion function were found by combining both methods. In contrast to our earlier paper with a similar hybrid acrylate-epoxy system, the treatment of the isokinetic relationship (IKR) is introduced in this work [9,12]. A correct discussion of the kinetic parameters requires the use of rate constant and isokinetic relationship (IKR) in order to eliminate the compensation effect between activation energy and pre-exponential factor. Model fitting was performed assuming that both thermal stages follow an autocatalytic model [13,14], and the selected model was confirmed by using IKR and integral master plots procedures. The isokinetic temperature derived from IKR was used to establish the dual nature of the formulations and the isothermal curing conditions.

Dynamic kinetic parameters were used to simulate the isothermal curing of both curing stages. The characterization of the whole set of cured materials and the quantification of the conversion were performed by calorimetry and Fourier-transform Infrared Spectroscopy (FTIR), respectively.

2 Experimental methods

2.1 Materials

The photocure resin was a commercial preparation supplied by Spot-A Materials (Barcelona, Spain) called Spot-E (abbreviated as E). It is a mixture of aliphatic and urethane acrylates that has an average molecular weight of 627 g/mol, and functionality 1.32. The preparation contains a photoinitiator with an absorption range in the UV-visible region of the spectrum. Diglycidyl ether of bisphenol A with trade name EBL 70 (DG hereafter) with an epoxy equivalent of 184.5 g/ee was kindly supplied by PO.INT.ER S.r.l (Turin, Italy). The anhydride component was hexahydro-4-methylphthalic anhydride (abbreviated as MA, 168.19 g/ea) supplied by Sigma-Aldrich. Before each use, the epoxy

resin EBL70 was placed in vacuum and dried at 80°C for 2h. The anionic initiator for the epoxy-anhydride reaction was 4-(dimethylamino)pyridine (DMAP, Sigma Aldrich) and the thermally-activated radical initiator was 1,1-di(t-amylperoxy)-cyclohexane with trade name LUPEROX 531M60 (LUP hereafter), supplied by ARKEMA (Colombes, France).

2.2 Sample preparation

Firstly, a stoichiometric epoxy-anhydride mixture containing DMAP at weight ratio DMAP/DGMA of 0.025/99.975 was prepared under magnetic agitation at 30 °C for 10 min until a clear solution was obtained. This was coded as DGMA100. For the acrylate part, LUP was taken to a glass vial or an opaque container and Spot-E was added on top. The weight ratio was $LUP/E = 0.25/99.75$ and the formulation was coded as E100. Formulations were prepared under ambient conditions and were coded as ExDGMA_y, where x and y stand for weight percentages of E100 and DGMA100, respectively. All samples were stored in opaque vials under refrigeration to avoid undesired photopolymerization. The characterized formulations were E100, E80DGMA20, E60DGMA40, E40DGMA60, E20DGMA80 and DGMA100. For curing kinetics analysis, only neat formulations and E40DGMA60 were studied. The choice of E40DGMA60 stems from our earlier work in which this formulation was shown to achieve a good balance between shape consistency at the intermediate curing stage and high glass transition temperature at the final stage [10]. For comparison purposes, a dual formulation E40DGMA60 without DMAP was also prepared and coded as E40DGMA60_noDMPA.

2.3 Experimental techniques

The Differential Scanning Calorimetry (DSC) analysis of photo-initiating formulations were carried out in a Mettler DSC-821e calorimeter featuring a Hamamatsu Lightningcure LC5 (Hg-Xe lamp) with irradiation intensity of 2 mW·cm⁻².

Approximately 3 mg of sample were cured in uncapped aluminum pans in a nitrogen atmosphere. Scans were repeated to be able to subtract the second scan from the first to eliminate the thermal effect of UV irradiation. Each run consisted of 1 min of temperature conditioning, followed by 6 min of irradiation, and an additional 1 min without irradiation. For the rest of the DSC analysis, we used a Mettler DSC 3+ calorimeter. Samples of approximately 10 mg were placed in aluminum pans and scanned in an inert atmosphere. Dual-curing samples were dynamically cured starting at -80 °C and ending at 300 °C. Heating rate was 10 K/min. This was done to determine T_g of uncured samples (T_{g0}) and the total polymerization heat (of the entire dual-cure). To measure intermediate T_g (T_{gint}) and the residual polymerization heat of stage 2, UV-cured samples were scanned in the same way as above, followed by a second dynamic scan to determine the final T_g ($T_{g\infty}$). The halfway point of heat capacity step was taken as T_g , as per the DIN 51007 standard method. The estimation error was $\pm 1^\circ\text{C}$.

For the study of kinetics, non-isothermal curing was performed at heating rates of 2.5, 5, 10 and 20 K/min up to 300 °C for the entire dual-curing and also for the second curing stage of intermediate materials. E100 formulation was also cured isothermally at 110, 120 and 130 °C (stage 1) and compared with the simulation from the results of the non-isothermal kinetics analysis in order to validate the methodology.

Polymerization heats were calculated by integrating the calorimetric signal, dh/dt . A relative conversion, α , is defined as follows:

$$\alpha = \frac{\Delta h_{t,T}}{\Delta h_{tot}} \quad (1)$$

where $\Delta h_{t,T}$ is the heat evolved by time t or up to a temperature T during isothermal and dynamic curing experiments, respectively. The total polymerization heat is Δh_{tot} . An absolute conversion of each monomer can be calculated by multiplying α by the component mole fraction.

For spectroscopic analysis, a Bruker Vertex 70 FTIR spectrometer was used which features an attenuated total reflection (ATR) apparatus (Golden gate™, Specac Ltd) and is temperature controlled (heated single-reflection diamond ATR crystal). Acrylate and anhydride conversion during isothermal dual-curing was monitored. Real-time spectra were collected at 30 °C (stage 1) and 150 °C (stage 2) in absorbance mode with a resolution of 4 cm⁻¹. The wavelength range was from 400 to 4000 cm⁻¹ and 20 scans were performed for each spectrum. The same UV lamp as in DSC analysis was used here as well. DSC non-isothermal kinetic data was used to simulate a tentative curing time for stage 2, as will be shown later.

The peaks at 1407 cm⁻¹ (CH₂ scissor deformation mode) and 1862-1785 cm⁻¹ (carbonyl stretching) were used to monitor acrylate and anhydride conversion, respectively, similar to previous works [9,11]

3 Theory

3.1 Photocuring

Assuming that photopolymerization is a first-order steady state polymerization at the initial stage, and since no autocatalysis takes place, the rate of polymerization can be defined as [15,16]:

$$-\frac{d[M]}{dt} = k_p \left(\frac{\phi_i \cdot I_a}{k_t} \right)^{1/2} [M] \quad (2)$$

The expression can be written in terms of conversion as follows:

$$\ln(1-\alpha) = -k t \quad (3)$$

where k is an apparent first-order rate constant, k_p and k_t are the propagation and termination rate constants, $[M]$ is the concentration of acrylate, ϕ_i is the photolysis quantum yield, and I_a is the absorbed light intensity. The product $\phi_i \cdot I_a$ gives the initiation rate.

The first-order rate constant k at 30 °C of all formulations were obtained from the slope of $\ln(1-\alpha)$ plotted against time t . Neither the activation energy nor any other kinetic parameter were determined.

3.2 Thermal curing

Isoconversional and model fitting methods, along with isokinetic relationship (IKR) and master plots procedures in their integral form were used to determine the kinetic parameters of thermal curing of E100, DGMA100 and E40DGMA60 [9,12,17].

The kinetics of non-isothermal curing were analyzed by means of Kissinger-Akahira-Sunose (KAS) method, based on the Coats-Redfern approximation for the solution of the so-called temperature integral [12,18,19]:

$$\ln\left(\frac{\beta_i}{T_{\alpha,i}^2}\right) = \ln\left[\frac{A_\alpha R}{g(\alpha) E_\alpha}\right] - \frac{E_\alpha}{RT_{\alpha,i}} \quad (4)$$

where A_α is the frequency factor, E_α the activation energy, R the gas constant and $g(\alpha)$ the integral conversion function obtained by integration of the differential function $f(\alpha)$.

The values of dynamic kinetic parameters E_α and $\ln[A_\alpha R / g(\alpha) E_\alpha]$, are determined from the slope and y-intercept of the plot of $\ln(\beta_i / T_{\alpha,i}^2)$ versus $1 / RT_{\alpha,i}$, respectively. If the reaction model $g(\alpha)$ is known, the corresponding pre-exponential factor can also be calculated. From the y-intercept, it is possible to obtain the parameter $\ln[g(\alpha) / A_\alpha]$ and simulate the isothermal time of curing to reach a given relative conversion at temperature $T_{\alpha,i}$, using the following equation which was calculated by integration of the rate equation in isothermal conditions:

$$\ln t_{\alpha,i} = \ln\left[\frac{g(\alpha)}{A_\alpha}\right] + \frac{E_\alpha}{RT_{\alpha,i}} \quad (5)$$

The reaction model was determined on the basis of a composite integral method using the following expression obtained by rearranging equation (4):

$$\ln\left(\frac{g(\alpha)\beta_i}{T^2}\right) = \ln\left[\frac{AR}{E}\right] - \frac{E}{RT} \quad (6)$$

Given that the curing of epoxy-anhydride and thermal acrylate homopolymerization show an autocatalytic-like behavior, using Equation (6), the experimental data from the whole conversion range and the whole set of heating rates were fitted to an autocatalytic kinetic model with $n + m = 2$, where n and m are the orders of reaction [9,13,14,17,20].

Eqs. (7) and (8) give $g(\alpha)$ and $f(\alpha)$ functions, for the autocatalytic kinetic model used:

$$g(\alpha) = \frac{1}{1-m} \left(\frac{\alpha}{1-\alpha}\right)^{1-m} \quad (7)$$

$$f(\alpha) = \alpha^m (1-\alpha)^{2-m} \quad (8)$$

Once the model was fixed by model fitting, rate constants k were determined from E and A by using the Arrhenius equation.

The activation energy and the pre-exponential factor may be linked, due to a compensation effect, through the following isokinetic relationship (IKR) [11,17,21,22]:

$$\ln A_\alpha = aE_\alpha + b \quad (9)$$

where a and b are constants and the subscript α refers to a change producing factor in the Arrhenius parameters (in our case, the conversion). The slope $a=1/RT_{\text{iso}}$ is a function of the isokinetic temperature T_{iso} and the y-intercept $b=\ln k_{\text{iso}}$ is the natural logarithm of the isokinetic rate constant. According to certain authors, the existence of the IKR demonstrates that only one mechanism is present, whereas the existence of parameters that do not agree with the IKR implies the existence of multiple reaction mechanisms or the proposed mechanism is not accurate. A T_{iso} value near the experimental temperature

range also indicates that the model is correct [12,17,21,22]. The kinetic model determined by model fitting was confirmed by the existence of IKR with a good regression coefficient for the whole kinetic data and also by values of T_{iso} . This methodology has proven to be adequate when the isoconversional activation energy varies only slightly with the extent of conversion.

Using $\alpha=0.5$ as a reference point, the following integral master equation is easily derived from Eq. (4):

$$\frac{g(\alpha)}{g(0.5)} = \frac{\exp\left(-\frac{E}{RT}\right)T^2}{\exp\left(-\frac{E}{RT_{0.5}}\right)T_{0.5}^2} \quad (10)$$

where $g(0.5)$ and $T_{0.5}$ are the integral conversion function and the reaction temperature at $\alpha=0.5$, respectively.

The left side of Eq. (10), is a reduced theoretical curve which is characteristic of each kinetic model. The right side of the equation can be obtained from constant heating rate experimental data if the activation energy is relatively constant throughout the reaction. The graphical comparison of both sides of Eq. (10), can be used to determine the kinetic model that best describes the curing process. In this work, this procedure has been used to confirm the model obtained by model fitting. An average value of the isoconversional activation energy has been used.

4 Results and discussion

4.1 Characterization of ExDGMAY formulations

To start, the sequential curing of E40DG60 formulation was studied under isothermal conditions (stage 1, UV at 30°C followed by stage 2 at 150 °C) by FTIR. Stage 2 temperature was selected based on the obtained kinetic data, as it will be shown later. Complete disappearance of absorption bands of acrylate (first curing stage) and epoxides

and anhydrides (second curing stage) was confirmed by FTIR analysis (spectra not shown here for space considerations).

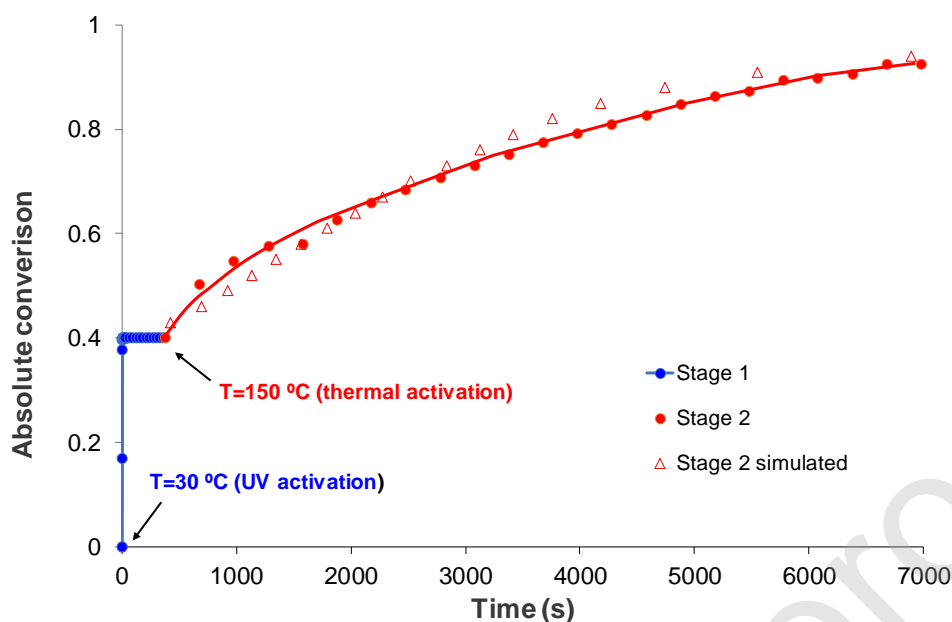


Fig. 1. FTIR absolute conversion during isothermal curing at 30 °C (stage 1, acrylate) and later at 150°C (stage 2, anhydride) for E40DGMA60. Simulation of stage 2 using non-isothermal kinetic parameters is also shown.

Fig. 1 shows the absolute conversions obtained from FTIR data. It can be observed that stage 1 reaches completion, indicated by a fractional conversion of 0.4, in only 6 seconds, whereas stage 2 completes in 140 minutes at 150°C. Epoxy and anhydride groups remain unreacted during photocuring at 30 °C (i.e. stage 1), and samples of intermediate stage material stored at 30 °C remain unchanged for at least 3 months. Moreover, stage 2 does not start unless the temperature is raised above 120 °C. This unequivocally confirms the sequential dual-curing character of ExDGMAy, which is controlled by irradiation/heating on demand.

Fig. 2 shows the results of the DSC analysis of the thermal curing of ExDGMAy formulations under non-isothermal conditions. The two disparate exotherms point to well-separated curing stages. They are associated to thermal acrylate homopolymerization and to epoxy/anhydride copolymerization, in increasing order of

temperature. Conversion-temperature curves also show two well-defined curing steps, with conversion increases paralleling the composition of formulations, corroborating the findings in FTIR analysis.

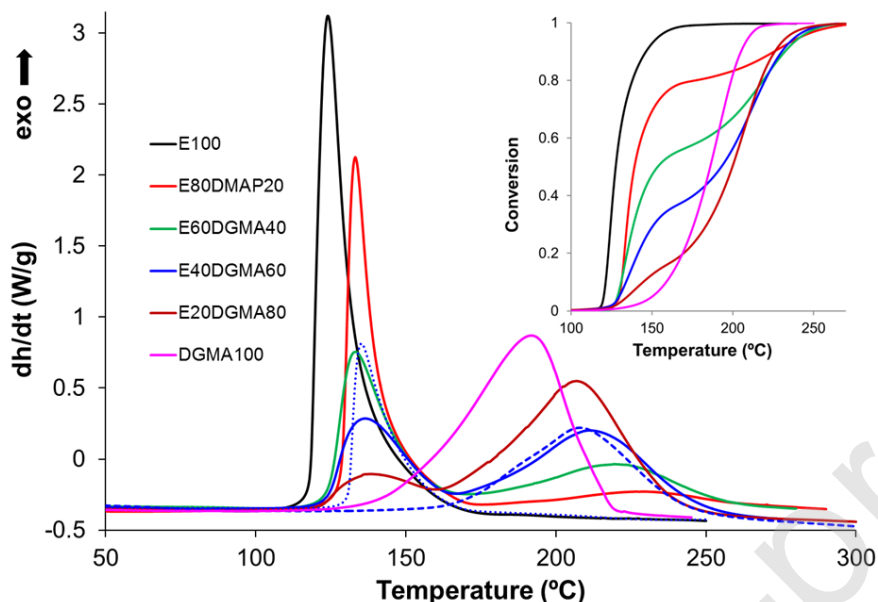


Fig. 2. DSC thermograms corresponding to the dynamic curing at 10 °C/min of ExDGMAy formulations. Blue dashed line shows the dynamic postcuring of E40DGMA60 after 6 min of UV irradiation. Blue dotted line shows curing of E40DGMA60_noDMPA. Inset: conversion-temperature plots.

Table 1 reports the reaction heat for the sequential dual-curing process. The individual values of the different curing stages were obtained by isothermal photocuring of the first curing stage followed by non-isothermal thermal curing of the second stage, Δh_1 and Δh_2 respectively. From reaction heats of neat formulations (E100 273 J/g and DGMA100 327 J/g) reported in **Table 1**, the following heats per reactive group have been determined: 129 kJ/C=C and 115 kJ/ee. These values are in agreement with those reported in the literature for similar systems [5,13]. A theoretical reaction heat of the dual-curing formulations was calculated from their composition and the reaction heat of the neat acrylate and epoxy/anhydride formulations. The similarity between theoretical and experimental reaction heats confirms again that the curing of all formulations have been complete (as has also been seen by FTIR). Moreover, the reaction heat obtained from the dual dynamic curing at 10 K/min in the absence of UV irradiation, Δh_{tot} , is close to the

sum of Δh_1 and Δh_2 , evidencing the ability of LUP to promote the complete thermal free radical polymerization of acrylate groups in the absence of irradiation. In addition, it is also suggested that it is possible to obtain the same material following different dual-curing procedures with controlled curing sequence.

Fig. 2 shows there is a deceleration effect exerted by liquid epoxy and anhydride on the first curing stage, which could be expected taking into account the dilution of the reactive species. DSC traces of E100 suggest that the minimum temperature necessary for the thermal activation of LUP is 110 °C. Once activated, the reaction rate increases sharply. In a previous work, in which a cycloaliphatic epoxy resin was used instead of DGEBA, a somewhat different effect was observed [9]. At low amounts of photocurable resin, DMAP exerted an accelerating effect on stage 1 due to the decomposition of LUP via chemical reduction and due to the nucleophilic addition of DMAP to the acrylate (Michael addition). Although this effect is not as clearly observed in this work, it should not be ruled out, since a comparison between the thermograms of E40DGMA60 and E40DGMA60_noDMAP might suggest the existence of such an effect (See Fig. 2).

On the other hand, **Fig. 2** also shows that the second stage curing process is shifted to higher temperatures with decreasing DGMA content. This reduction in the reaction rate of the second curing stage can be ascribed to a dilution of the epoxy-anhydride components, but also to further restriction in the mobility caused by the previous formation of the acrylate network. Moreover, it can be seen in **Fig. 2** that stage 2 curing of E40DGMA60 is identical regardless of how stage 1 is carried out (compare the blue solid and dashed lines). In any dual formulation, stage 2 starts only above 150 °C. Taking into consideration this preliminary analysis of the sequential dual-curing kinetics and the previous discussion on the reaction heat values reported in **Table 1**, a perfectly sequential

and fully controllable curing process is established for our ExDGMAy family of materials.

Table 1 also reports the glass transition temperatures of uncured, intermediate and fully cured ExDGMAy formulations. The T_g of unreacted dual materials vary in accordance with the T_g of their neat components. The T_g of intermediate materials (after stage 1) decrease with increasing DGMA content, due to the plasticizing effect of the liquid unreacted DGMA. Not surprisingly, in all formulations, a significant increase in T_g is recorded after stage 2, the increase being proportional to the DGMA content. The fully cured materials have increasing T_g with increasing DGMA content, due to the high degree of crosslinking and rigidity of epoxy-anhydride network in comparison to the acrylate network. Thermal characteristics of the intermediate and final materials can be tuned by simply modifying the initial composition, to obtain loosely or tightly crosslinked thermosets. Intermediate materials can be used as adhesives or manipulated to create complex shaped objects with shape memory properties after being fully cured. In general, all dual formulations seem apt for 3D printing applications. Intermediate T_g below room temperature ensure low shrinkage and that no vitrification takes place during printing. Final T_g above room temperature ensure glassy materials with high modulus at room temperature, which are desirable operation conditions for these materials. In a previous work, the shape memory capability of the E40DGMA60 formulation was demonstrated [11]. After the partially-cured material was 3-D printed, it could be molded into its desired permanent form, which could be fixed by a thermal cure. Temporary shape fixing and shape recovery cycles could be implemented through facile heating-cooling programs featuring easily accessible temperatures.

4.2 Kinetic analysis

4.2.1. Photocuring of ExDGMAy

Firstly, the photocuring kinetics of all ExDGMAy formulations were studied by DSC. **Fig. 3** shows curing rate and conversion curves obtained from isothermal photoDSC runs at 30 °C. The photocuring of all formulations completes in just two minutes with a sharp curing profile, especially at the initial stage.

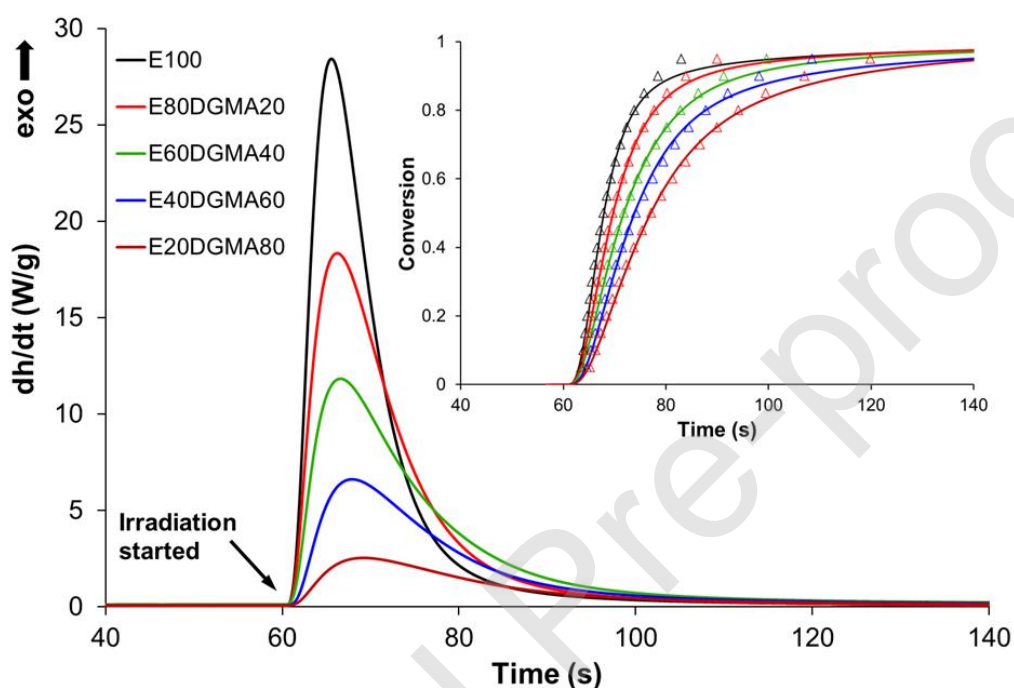


Fig. 3. Reaction rate for the isothermal UV-curing at 30 °C of ExDGMAy formulations. Inset shows conversions against time (the colour mapping is the same) and triangles represent simulated data using first-order constant and Eq. (3).

It was confirmed by FTIR that acrylates react completely, whereas epoxy and anhydride groups do not react during irradiation. The addition of the DGMA mixture to the photoresin decelerates the curing, due to a dilution effect.

First-order rate constants, obtained by using Eq. (3) from conversions and times (inset **Fig. 3**), are collected in **Table 2**. They reflect the decelerating effect exerted by DGMA. Correlation coefficients show an excellent fit in the same way as simulated data, even out of the range in which the kinetic parameters were obtained. This validates the

methodology used. **Fig. 3** and the values reported in **Table 2** do not suggest any evidence of the influence of DMAP on the first stage of curing, contrary to what was reported in a previous article **Error! Reference source not found.**. Indeed, taking Eq. (2) as a reference, and assuming that the absorbed intensity I is proportional to the initiator content and therefore to the fraction of acrylate formulation in the dual-curing systems, it can be observed that the kinetic constant k is proportional to $I^{0.68}$, which is very similar to the results reported by other authors for 3D-printable acrylate formulations [5].

4.2.2 Non-isothermal curing of neat formulations

First of all, the kinetics of non-isothermal curing of neat formulations was studied, E100 and DGMA100. **Fig. 4** gives the resulting DSC traces of both formulations.

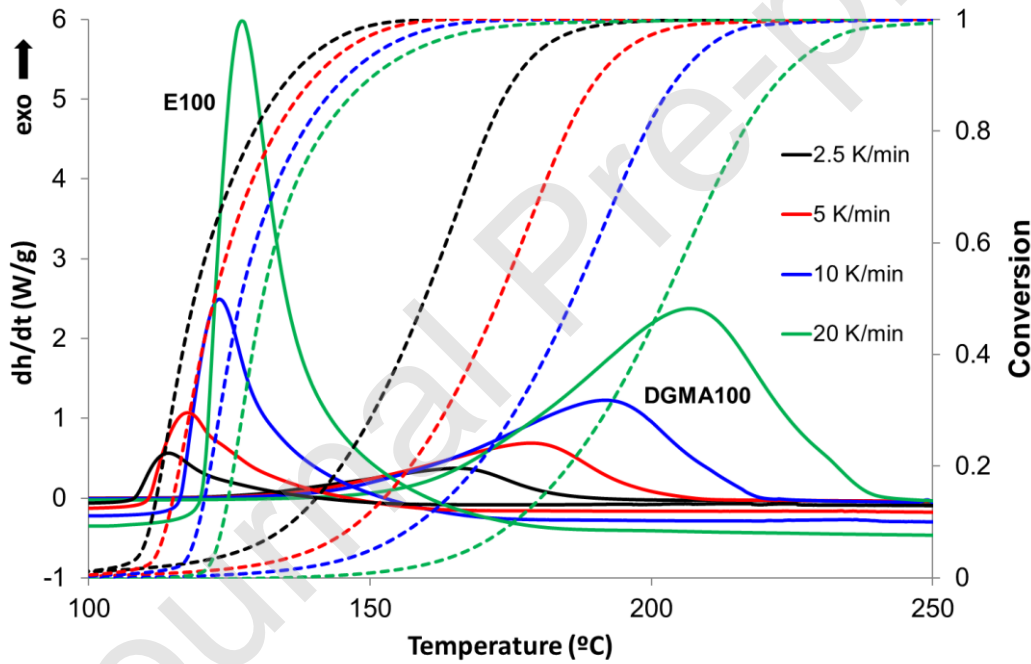


Fig. 4. DSC thermograms (solid lines) and conversions (dashed lines) of E100 and DGMA100, non-isothermally cured at different heating rates.

It can be seen that the curing of each formulation takes place in a completely different temperature range with only a slight overlap in a region of intermediate temperatures. Moreover, the curing behavior of DGMA100 is more sensitive to temperature than that

of E100. These results suggest that each system has unique kinetics and that with a suitable selection of temperatures, a completely sequential thermal curing can be achieved in dual formulations. In addition, in these formulations, all unreacted acrylates remaining from a 3D-printing stage will thermally cure, concurrently with the epoxy-anhydride reaction, thanks to the thermally initiated radical generator employed.

Using the data shown in **Fig. 4** in isoconversional analysis and model fitting (autocatalytic model with $n + m = 2$) (Eqs. (4), (6) and (7)), the curing kinetics was investigated. **Tables 3, 4, 5** and **6** show the results obtained for both neat formulations. Activation energy and pre-exponential factor are fairly constant throughout the curing with some minor variations without any physicochemical implications. Furthermore, the values are similar to those obtained by model fitting. These results, along regression coefficients close to unity, confirm the reliability of our methodology. It is observed that activation energies of E100 are slightly higher than other unsaturated systems where a thermal radical initiator less latent than LUP is used [17,23,24]. The kinetic triplet (E , A , $g(\alpha)$) associated to the curing of DGMA100 is similar to that obtained for other epoxy-anhydride systems activated by tertiary amines [19,25,26].

It is common in the literature to use activation energy (E) for reactivity comparison purposes, given that systems with high E react more slowly than those with low E . This reasoning can be valid in many cases, unless a compensation effect exists between the E and the pre-exponential factor (A). Thus, a system with high E can react faster than another with lower E if A is also high. To avoid misinterpretation, it is more appropriate to use the rate constant k as a comparison parameter since it includes the effects of both parameters, E and A . In consequence, the reactivities of the two curing stages were compared from the value of k at 150 °C ($k_{150\text{ °C}}$, see Tables 3-6). Although the E of E100 is higher than that of DGMA100, the rate constants show the opposite trend. $k_{150\text{ °C}}$ of

E100 is more than 300 times greater than $k_{150\text{ }^\circ\text{C}}$ of DGMA100, in accordance with the much lower thermal reactivity of the epoxy/anhydride mixture. The strongly different reactivity of the two curing stages highlights the dual nature of the ExDGMAy mixtures. This will be confirmed later in the study of curing kinetics of a dual formulation, where the mutual dilution effect enhances the sequential character of the curing process (see **Fig. 2**).

Values of $k_{30\text{ }^\circ\text{C}}$ allow comparison of the curing stages and the mechanisms of activation (see Tables 2, 4 and 6). The great difference of $k_{30\text{ }^\circ\text{C}}$ between 9.1 min^{-1} for E100 (neat stage 1, UV activated) and $3.4 \cdot 10^{-5}\text{ min}^{-1}$ for DGMA100 (neat stage 2, thermal activated) hints the high storage stability of the ExDGMAy mixtures at $30\text{ }^\circ\text{C}$ and the feasibility of their sequential processing (UV irradiation, followed by thermal activation). Moreover, the value of $k_{30\text{ }^\circ\text{C}}=2.98 \cdot 10^{-9}\text{ min}^{-1}$ for E100 (thermal) indicates that the addition of the highly latent LUP does not endanger the storage stability of the formulations.

In **Fig. 5**, the simulation of isothermal cure of E100 is shown in comparison to experimental data. The simulation was performed using non-isothermal parameters of **Table 3** and Eq.(5). The selection of temperatures was difficult since below $110\text{ }^\circ\text{C}$ the curing hardly commences and above $130\text{ }^\circ\text{C}$ it is extremely fast. As can be seen in **Fig. 5**, the simulated curves fit reasonably well with experimental data, in spite of the uncertainty in the determination of the reaction heat under isothermal conditions at the beginning and at the end of the curing process. In any case, the use of dynamic DSC data, obtained in a relatively simple way, is a useful and fairly accurate tool for estimating isothermal curing times, which are usually more difficult to obtain.

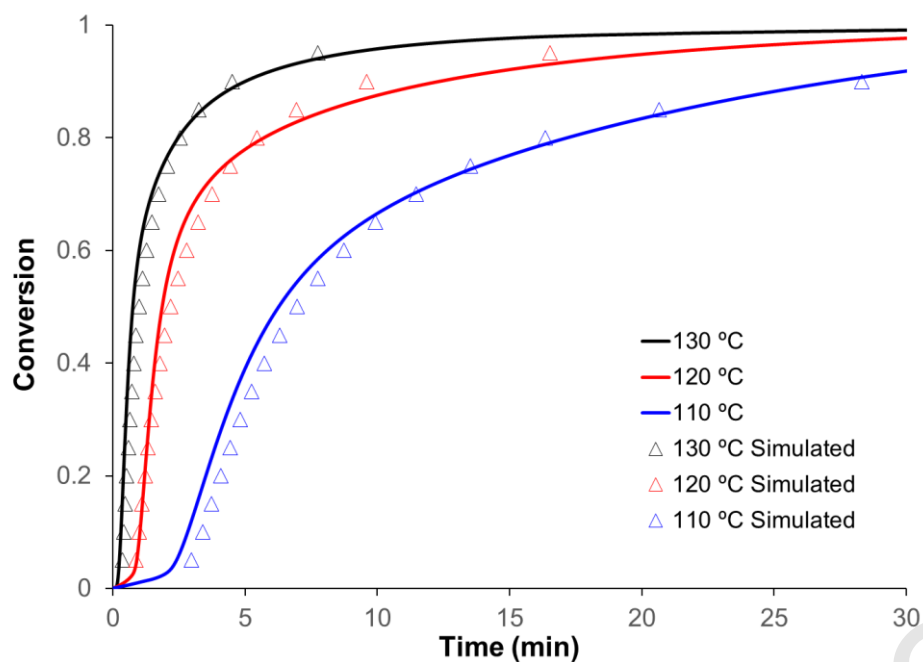


Fig. 5. Conversions against time for isothermal curing of E100 at different temperatures. Triangles represent simulated data using non-isothermal data of Table 3 and Eq. (5).

4.2.3. Non-isothermal dual curing of E40DGMA60

As a proof of concept, E40DGMA60 formulation was selected to study the dual-curing kinetics. **Fig.6** shows thermograms and conversions at different heating rate. The kinetic data obtained by isoconversional method and model fitting are given, in respective order, in **Tables 7** and **8**. Despite a clear sequence of stages, some overlapping is observed which might bias the determination of the kinetic parameters. Therefore, isoconversional data at 0.4 are not included.

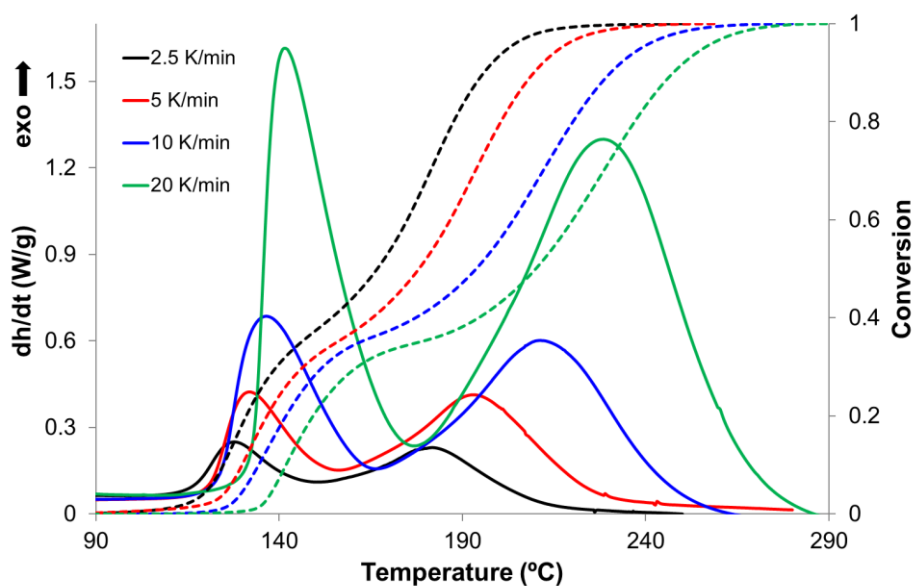


Fig. 6. DSC thermograms (solid lines) and relative conversion (dashed lines) of E40DGMA60 at different heating rates.

The results reported in **Tables 7** and **8** confirm the difference between the kinetics of the two thermal curing stages, as is also evident from **Fig. 6**. Again, due the compensation effect between E and A , the rate constant should be used to compare the kinetics ($k_{150\text{ }^{\circ}\text{C}}$, $stage\ 1$ is much higher $k_{150\text{ }^{\circ}\text{C}}$, $stage\ 2$).

The kinetic parameters obtained are consistent with those obtained previously for E100 and DGMA100. The dilution effect of liquid DGMA on radical homopolymerization as well as the mobility restrictions exerted by the acrylic network on epoxy-anhydride copolymerization, shown previously in **Fig. 2**, are corroborated by comparing $k_{150\text{ }^{\circ}\text{C}}$ of neat and dual formulations (see **Tables 4, 6** and **8**). $k_{150\text{ }^{\circ}\text{C}}=2.59\text{ cm}^{-1}$ of E40DGMA60 (stage 1) is much lower than $k_{150\text{ }^{\circ}\text{C}}=38.9\text{ cm}^{-1}$ of E100 whereas $k_{150\text{ }^{\circ}\text{C}}=0.081\text{ cm}^{-1}$ of E40DGMA60 (stage 2) is nearly half of $k_{150\text{ }^{\circ}\text{C}}=0.16\text{ cm}^{-1}$ of DGMA100.

Although the obtained kinetic parameters of the dual formulations are correct as indicated by the regression coefficients, the overlapping between stages conceal their

exact kinetics. In some regions, the parameters should be considered as average values of the two stages and will depend on the composition of the formulation and the degree of overlap. To determine a more accurate kinetic triplet of each stage, the following two strategies are proposed: 1- The deconvolution of the dynamic DSC peaks and, 2- photocuring the formulations followed by non-isothermal postcuring of the intermediate materials. The latter strategy is only applicable to curing stage 2. In both cases, the isoconversional methodology and model fitting will be applied.

Fig. 7 shows the partial overlapping between the curing stages and the deconvolution performed for E40DGMA60 at 2.5 K/min using the curve-fitting method with the Gaussian–Lorentzian sum area function of the program PeakFit (Jandel Scientific Software, San Rafael). A good fit can be observed between the experimental curve and the curve obtained as a sum of the deconvoluted ones.

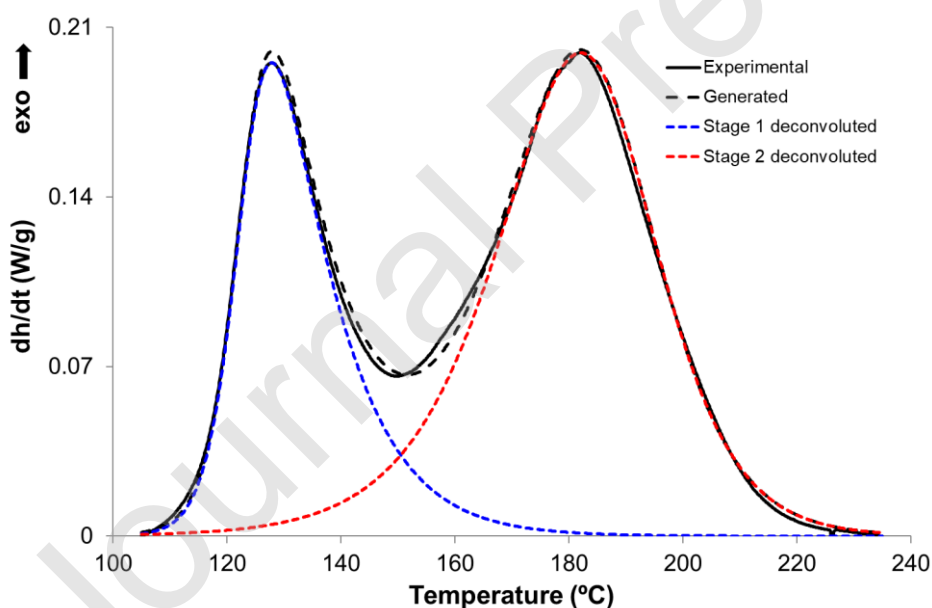


Fig. 7. DSC thermograms, curves obtained by deconvolution and the sum of the deconvoluted curves for E40DGMA60 cured at 2.5 K/min.

Fig. 8 shows the conversion curves obtained by integration of the deconvoluted peaks from the experimental data at 2.5, 5, 10 and 20 K/min. Even though there appears to be a region where both stages can take place concurrently (around 120-150 °C), the curing

stages take place in completely different temperature regions and at different reaction rates. This suggests that a careful temperature selection would allow a perfectly sequential curing. **Tables 9** and **10** show kinetic parameters obtained from the curves of **Fig.8**, that can be used to establish tentative cure conditions.

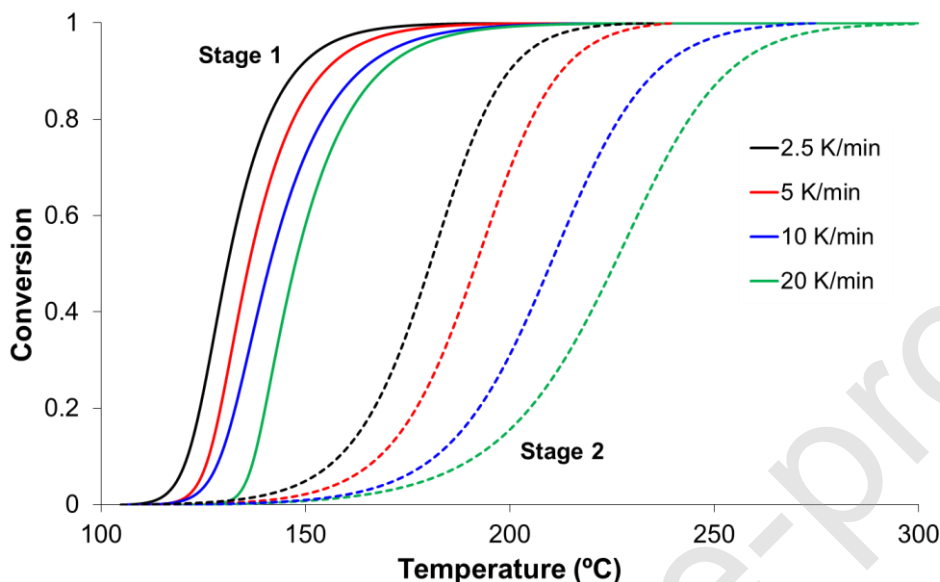


Fig. 8. Relative conversion at deconvoluted stages (stage 1 solid lines and stage 2 dashed lines) against temperature for E40DGMA60 at different heating rates.

Tables 9 and **10** show the results that are equivalent to those obtained directly by dual curing (**Tables 7** and **8**), although they must be considered more accurate since the overlap between stages has been eliminated. Regression coefficients ranged between 0.9998 for stage 1 and 0.9962 for stage 2 (not shown for space considerations).

It is noticeable that the kinetic models obtained from the analysis of stage 1 and stage 2 in the E40DGMA60 formulation are very similar to the ones obtained from the independent analysis of neat E100 and DGMA100 formulations. These results suggest that there is little interference between the first and second curing stage components, other than a dilution effect producing a decrease in the curing rate of the dual-curing formulation.

4.2.4 Stage 2 non-isothermal curing of E40DGMA60 after UV irradiation

In order to study the overlap-free stage 2 of dual-curing, E40DGMA60 formulation was firstly cured at 30 °C (stage 1 only). After that, it was dynamically scanned to isolate stage 2. **Fig. 9** shows heat flows and conversions versus temperature at different heating rates. As anticipated, the DSC peak appeared at the same temperature range as stage 2 of non-isothermal dual-curing without deconvolution (see **Fig. 6**) or after deconvolution (see **Fig. 8**). The fact that no stage 2 reaction takes place during UV irradiation suggests that the parameters obtained in this section should be the most reliable. Moreover, this methodology yields much better regressions and the kinetic parameters are more constant throughout the conversion range, indicating that the fluctuations detected in dual curing (with or without deconvolution) can be attributed to mathematical artifacts and not to appreciable kinetic changes, as it will be proven with the help of isokinetic relations.

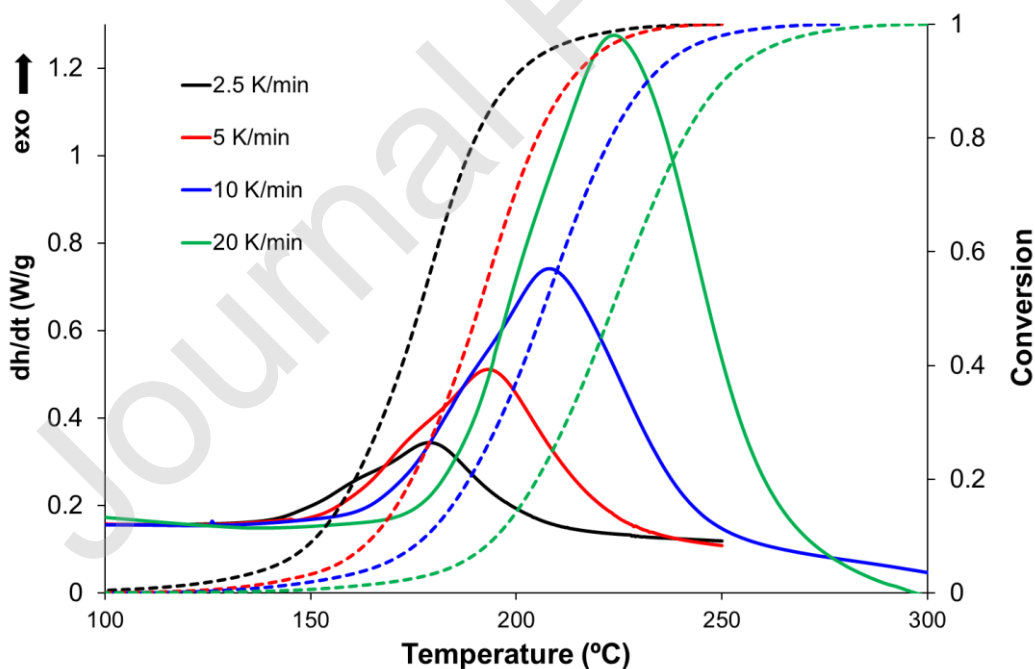


Fig. 9. DSC thermograms (solid lines) and relative conversion (dashed lines) of E40DGMA60 at different heating rates after photocuring at 30 °C.

Tables 11 and **12** show the kinetic parameters associated to stage 2. If the values are compared with the ones reported in **Tables 9** and **10**, an excellent agreement is observed, which confirms the validity of the methodology used. The kinetic parameters in **Table 11** were used in Eq. (5) to simulate the isothermal curing at 150 °C, with reasonably good results, as is shown in **Fig. 1**.

4.2.5. Validation of the kinetic model

Identifying an appropriate model is of paramount importance in model fitting. If this is not done correctly, the kinetic parameters will be meaningless. According to the literature and our previous works, an autocatalytic model with $n+m=2$ is assumed for both thermal curing stages. The application of the model-fitting methodology produced highly consistent results regardless of the specific method employed, i.e. regardless of the treatment of experimental data. It was also noticeable that the kinetic model governing the first and second curing stages was hardly affected by the dilution effect in the dual-curing formulation in comparison with the neat E100 and DGMA100 formulations. In this section, further validation of the model is provided by means of a graphical method based on master plots, which can be used to visually establish the correct model prior to numerical fitting in order to obtain the exact parameters. Moreover, the relative reactivity of the different curing stages and the feasibility of the sequential dual-curing scheme are reinterpreted in terms of the IKR relationships.

First of all, the integral reduced master plots shown in **Fig. 13** were used. In this plot, the theoretical curves are given for a set of usual kinetic models (power, D3, A3, R3, $n+m=2$) [11,16,26] and compared with experimental data. It can be seen that both stages fit well with an autocatalytic model ($n+m=2$) with n close to 1.7-1.8 and 1.5 for stage 1

and stage 2, respectively. Thus, it can be easily observed that other types of models should be completely discarded. Moreover, good starting values of the kinetic parameters for the numerical fitting method can be easily obtained.

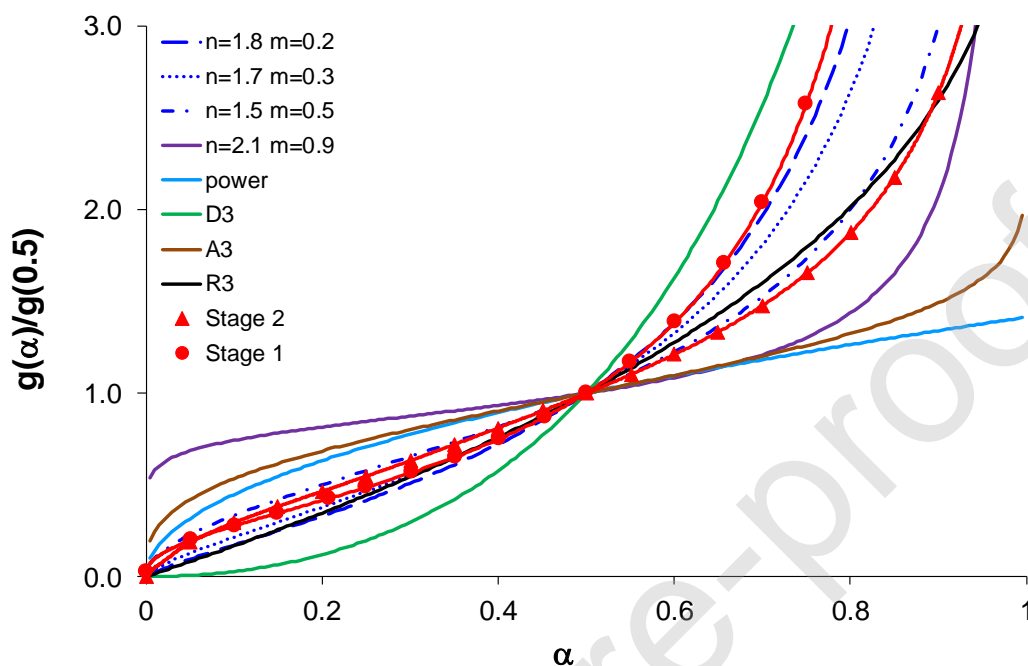


Fig. 10. A comparison of the theoretical integral master plots of $g(\alpha)/g(0.5)$ versus α with the experimental master curve at 10 K/min for E40DGMA60 dual formulation. Experimental data of stage 1 corresponds to the deconvoluted curve and of the stage 2 to the formulation cured after UV curing.

Finally, the kinetic model and the dual nature of formulation were validated by using isoconversional activation energies and pre-exponential factors and the isokinetic relationship (IKR). Regardless of the formulation or the methodology used, the kinetic model hardly varies at any stage. **Fig. 11** shows the IKR plots for all data obtained (**Tables 3, 5, 7, 9 and 11**). As can be seen, the kinetic data are perfectly grouped in two IKRs in different regions of the plot, according to the different reactivity of both stages. These results suggest that the selected model is correct and that some changes in the activation energies observed should be attributed to experimental fluctuations, rather than any mechanism changes. It should be noted that a variation of the activation energy near the

isokinetic temperature, T_{iso} , lead to a quasi-invariant rate constant, enabling different values of activation energy to represent the same kinetic event [27].

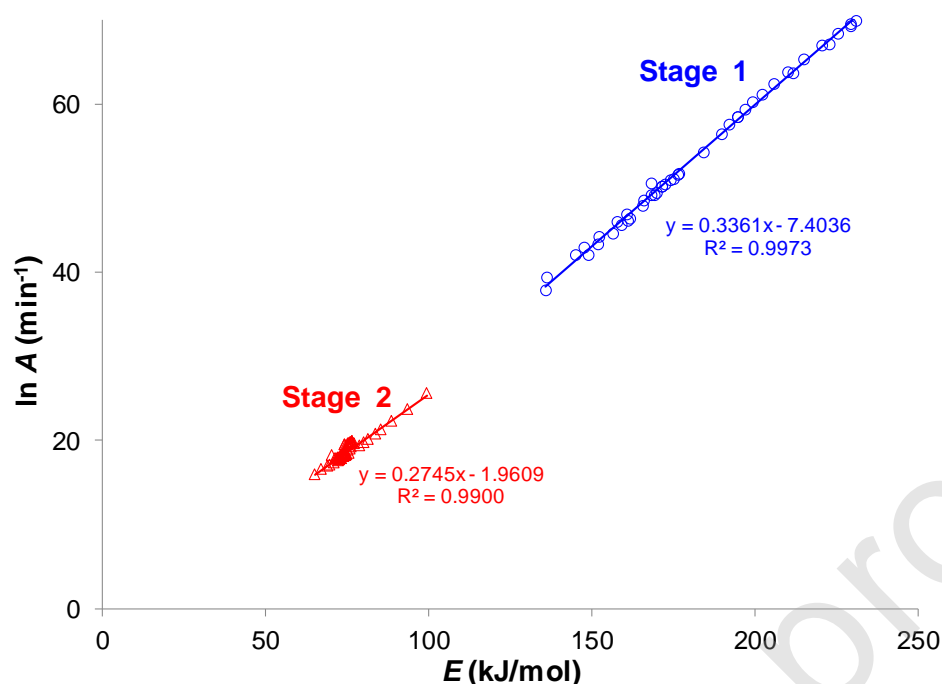


Fig. 11. Isokinetic relationships (IKRs) associated with each curing stage for the $n+m=2$ model. For stage 1, data from E100 and E40DGMA60 (dual and dual deconvoluted) are grouped. For stage 2, data from DGMA100 and E40DGMA60 (dual, dual deconvoluted and neat stage 2 after stage 1 UV) are grouped.

Although IKRs regression coefficients are high (see **Fig. 11**), a more accurate discussion, following the perspective of T_{iso} , is reached without grouping all data in only two IKRs. **Table 13** shows the IKRs of neat formulations and of stage 1 and 2 of E40DGMA60. The deconvoluted kinetic data from the curing of E40DGMA60 (**Table 9**, stage 1) and data from the stage 2 curing of the same formulation after photocuring at 30 °C (**Table 11**) were selected to represent stage 1 and 2, respectively, and were used to determine the IKRs of **Table 13**.

The good regression of IKRs and their T_{iso} within the experimental temperature range validate the kinetic model selected by model fitting [21,28]. Moreover, the values of T_{iso} are related to the reactivity of the formulation and they help rationalize the kinetic effects observed in this work. Low values of T_{iso} indicate higher reactivity since the curing can take place at lower temperatures. From data in **Table 13**, one can see the higher reactivity

of stage 1 in comparison with stage 2 and the strongly sequential character of the thermal dual curing ($T_{iso,stage 1} \ll T_{iso,stage 2}$). The mutual deceleration effect is also evident from the increase of T_{iso} of E40DGMA60 from 103 to 121 °C (stage 1) and from 167 to 218 °C (stage 2), with respect to the neat formulations.

5 Conclusions

The dual-cure kinetics of a new family of ternary acrylate/epoxy/anhydride thermosets is investigated. The two sequential steps are acrylate radical polymerization initiated by UV or heat, followed by thermal epoxy-anhydride copolymerization at higher temperatures. A first order model satisfactorily fits photocuring kinetics. The thermal curing was studied by isoconversional, model fitting, reduced master plot and isokinetic relationship methodologies.

The sequentiality of the dual curing process and the storage stability of the initial and intermediate materials was proven by the obtained kinetic data, which suggested different rate constants for acrylate homopolymerization and epoxy-anhydride reaction. Through a suitable selection of temperatures for each stage, a well-defined curing sequence without overlapping between curing stages can be obtained. Stage 1 can be initiated by UV irradiation and stage 2 can be initiated thermally. If a thermal radical initiator is used, stage 1 can be initiated thermally as well. This initiator would also allow complete curing of the acrylate groups during stage 2. This is especially relevant if these formulations are used in 3D printing, in which, generally, the conversions achieved are incomplete and non-uniform throughout the printing geometry.

The addition of an epoxy-anhydride component contributed greatly to mechanical performance, manifested as significant glass transition temperature increases over the neat acrylate photoresin. Prepared materials show a wide range of properties, with highly

flexible and shape-conformable intermediate materials and highly crosslinked, solid final materials.

Among the different kinetic methods used, the isoconversional method allows a relatively precise determination of the activation energy and an accurate simulation of the curing, even at temperatures fairly outside the experimental range. Moreover, this is accomplished without requiring any well-defined kinetic model. Due to the compensation effect between the activation energy and the pre-exponential factor, the use of the rate constant is advocated, since it takes into account both parameters as proxies of reactivity. In this case, the kinetic model would be required, which, unless previously known, can be constructed using the reduced master curves and then refined by means of model fitting.

Isokinetic relationship and the associated isokinetic temperature are other useful tools that allow the determination of the kinetic model and to elucidate whether the changes observed in the kinetic parameters during cure are due to mechanistic changes or due to the compensation effect. The isokinetic temperature also has reactivity implications: low isokinetic temperatures suggest high reactivity. In fact, this parameter can be extremely useful in dual curing. A highly sequential curing is expected when the isokinetic temperature of the stages is greatly different.

Author statement

Osman Konuray: Writing - review & editing, Visualization, Data curation, Conceptualization, Methodology, Software. José M. Morancho: Visualization, Investigation. Xavier Fernández-Francos: Data curation, Writing - original draft, Conceptualization, Methodology, Software. Montserrat García-Alvarez: Visualization, Investigation. Xavier Ramis: Project administration, Writing - review & editing, Supervision, Data curation, Writing - original draft, conceptualization, Methodology, Software.

Declaration of interests

The authors declare that they have no known competing financial interests or personal relationships that could have appeared to influence the work reported in this paper.

Acknowledgments

The authors would like to thank MCIU (Ministerio de Ciencia, Innovación y Universidades) (MAT2017-82849-C2-2-R), FEDER (Fondo Europeo de Desarrollo Regional) (MAT2017-82849-C2-2-R and BASE3D) and Generalitat de Catalunya-Secretaria d'Universitats i Recerca (BASE3D, 2017-SGR-77) for the financial support. Xavier F.-F. also acknowledges the Serra-Hünter programme (Generalitat de Catalunya). The authors would also like to thank Spot-A Materials for supplying the Spot E, and PO.INT.ER S.r.l for supplying the epoxy resin.

References

- [1] T.D.Ngo, A. Kashani, G. Imbalzano, K.T.Q. Nguyen, D. Hui, Additive manufacturing (3D printing): A review of materials, methods, applications and challenges, *Compos B Eng*, 117 (2018) 172-196. <https://doi.org/10.1016/j.compositesb.2018.02.012>.
- [2] S.C. Ligon, R. Liska, J. Stampfl, M. Gurr, R. Mülhaupt, Polymers for 3D printing and customized additive manufacturing, *Chemical Reviews* 117 (2017) 10212-10290. <https://doi.org/10.1021/acs.chemrev.7b00074>.
- [3] M. Hofmann, 3D printing gets a boost and opportunities with polymer materials. *ACS Macro Letters*, 3 (2014) 382–386. <https://doi.org/10.1021/mz4006556>.
- [4] G. Taormina, C. Sciancalepore, M. Messori, 3D printing processes for photocurable polymeric materials: technologies, materials, and future trends, *J. Appl. Biomater. Funct. Mater.* 16 (2018) 151-160. <https://doi-org/10.1177/2280800018764770>
- [5] A.C. Uzcategui, A.Muralidharan, V.L. Ferguson, S.J. Bryant, R.R. McLeod, Understanding and Improving Mechanical Properties in 3D printed Parts Using a Dual-Cure Acrylate-Based Resin for Stereolithography, *Adv. Eng. Mater.* 20 (2018) 1800876. <https://doi.org/10.1002/adem.201800876>.
- [6] G. Griffini, M. Invernizzi, M. Levi, G. Natale, G. Postiglione, S. Turri, 3D-printable CFR polymer composites with dual-cure sequential IPNs. 91 (2016) 174-179. <https://doi.org/10.1016/j.polymer.2016.03.048>.
- [7] X. Kuang, Z. Zhao, K. Chen, D. Fang, G. Kang, H.J. Qi, High-Speed 3D Printing of High-Performance Thermosetting Polymers via Two-Stage Curing, *Macromol. Rapid. Commun.* 39 (2018) 1700809. <https://doi.org/10.1002/marc.201700809>.
- [8] O. Konuray, F. Di Donato, M. Sangermano, J. Bonada, A. Tercjak, X. Fernández-Francos, À. Serra, X. Ramis, Dual-curable stereolithography resins for superior thermomechanical properties, *Express Polym. Lett.* 14 (2020) 881–894. <https://doi.org/https://doi.org/10.3144/expresspolymlett.2020.72>.

- [9] O. Konuray, J.M. Salla, J.M. Morancho, X. Fernández-Francosa, M. García-Alvarez, X. Ramis, Curing kinetics of acrylate-based and 3D printable IPNs, *Thermochim. Acta* 692 (2020) 178754. <https://doi.org/10.1016/j.tca.2020.178754>
- [10] A. Gupta, A.A. Ogale, Dual curing of carbon fiber reinforced photoresins for rapid prototyping, *Polym. Com.* 23 (2002) 1162-1170. <https://doi.org/10.1002/pc.10509>.
- [11] O. Konuray, A. Sola, J. Bonada, A. Tercjak, X. Fernández-francos, X. Ramis, Cost-effectively 3D-printed rigid IPNs with shape memory capability, *Materials*, under revision.
- [12] S. Vyazovkin, A.K. Burnham, J.M. Criado, L.A. Pérez-Maqueda, C. Popescu, N. Sbirrazzuoli ICTAC Kinetics Committee recommendations for performing kinetic computations on thermal analysis data, *Thermochim. Acta* 520 (2011) 1-19. doi:10.1016/j.tca.2011.03.034.
- [13] M. Flores, X. Fernández-Francos, X. Ramis, A. Serra, Novel epoxy-anhydride thermosets modified with a hyperbranched polyester as toughness enhancer. I. Kinetics study, *Thermochim. Acta* 544 (2012) 17-26. <http://dx.doi.org/10.1016/j.tca.2012.06.00>
- [14] F. Shokrolahi, M. Zandi, P. Shokrollah, M. Atai, E. Ghafarzadeh, M. Hanifeh, Cure kinetic study of methacrylate-POSS copolymers for ocular lens, *Pro. Biomater.* 6 (2017) 147-156. <https://doi.org/10.1007/s40204-017-0074-x>.
- [15] C. Decker, Kinetic Study and New Applications of UV Radiation Curing, *Macromol. Rapid Commun.* 23 (2002) 1067-1093. <http://dx.doi.org/10.1002/marc.200290014>.
- [16] J.-S. Kim, .S.-T. Noh, J.-O. Kweon, B.-S. Cho, Photopolymerization kinetic studies of UV-curable sulfur-containing difunctional acrylate monomers using photo-DSC, *Macromol. Research.* 23 (2015) 341-349.
- [17] A. Cadenato, J. M. Morancho, X. Fernández-Francos, J. M. Salla, X. Ramis, Comparative kinetic study of the non-isothermal thermal curing of bis-GMA/TEGDMA systems, *J. Thermal Anal. Cal.* 89 (2007) 233-244. <https://doi.org/10.1007/s10973-006-7567-5>.
- [18] T. Akahira, T. Sunose, Method of determining activation deterioration constant of electrical insulating materials, *Res. Report Chiba Inst. Technol. (Sci. Technol.)* 16 (1971) 22-31.
- [19] A.W. Coats and J.P. Redfern, Kinetic Parameters from Thermogravimetric Data, *Nature* 207 (1964) 68-69. <http://dx.doi.org/10.1038/201068a0>.

- [20] J. Masson *Acrylic Fiber Technology and Applications* CRC Press, Cleveland 1995.
- [21] S. Vyazovkin, W. Linert, False isokinetic relationships found in the nonisothermal decomposition of solids, *Chem. Phys.*, 193 (1995) 109-118. [https://doi.org/10.1016/0301-0104\(94\)00402-V](https://doi.org/10.1016/0301-0104(94)00402-V).
- [22] S. Vyazovkin, W. Linert, The Application of Isoconversional Methods for Analyzing Isokinetic Relationships Occurring at Thermal Decomposition of Solids, *J. Solid State Chem.*, 114 (1995) 392-398. <https://doi.org/10.1006/jssc.1995.1060>.
- [23] J.M. Salla, X. Ramis, Comparative Study of the Cure Kinetics of an Unsaturated Polyester Resin Using Different Procedures, *Polym. Eng. Sci.* 36 (1996) 835-851. <https://doi.org/10.1002/pen.10471>.
- [24] J. M. Morancho, A. Cadenato, X. Fernández-Francos, J. M. Salla and X. Ramis, Isothermal kinetics of photopolymerization and thermal polymerization of bis-GMA/TEGDMA resins, *J. Thermal. Anal. Cal.* 92 (2008) 513-522. doi: 10.1007/s10973-007-8432-x.
- [25] J.M. Morancho, X. Fernández-Francos, C. Acebo, X. Ramis, J.M. Salla, A Serra, Thermal curing of an epoxy-anhydride system modified with hyperbranched poly(ethylene imine)s with different terminal groups, *J. Therm. Anal. Calorim.* 127 (2017) 645-654. doi: 10.1007/s10973-016-5376-z.
- [26] S. Montserrat, G. Andreu, P. Cortés, Y. Calventus, P. Colomer, J.M. Hutchinson, J. Malek, Addition of a reactive diluent to a catalyzed epoxy-anhydride system. I. Influence on the cure kinetics, *J Appl Polym Sci.* 61 (1996) 1663-674. [https://doi.org/10.1002/\(SICI\)1097-4628\(19960906\)61:10<1663::AID-APP6>3.0.CO;2-E](https://doi.org/10.1002/(SICI)1097-4628(19960906)61:10<1663::AID-APP6>3.0.CO;2-E).
- [27] X. Ramis, J.M. Salla, C. Mas, A. Mantecón, A. Serra, Kinetic Study by FTIR, TMA, and DSC of the Curing of a Mixture of DGEBA Resin and γ -Butyrolactone Catalyzed by Ytterbium Triflate, *J. Appl. Polym. Sci.* 92 (2004) 381–393. <https://doi.org/10.1002/app.20061>.
- [28] M. Arasa, X. Ramis, J.M. Salla, A. Mantecón, A. Serra, Kinetic study by FTIR and DSC on the cationic curing of a DGEBA/ γ -valerolactone, *Thermochim. Acta* 479 (2008) 37-44. doi:10.1016/j.tca.2008.09.020

Table 1. Reaction heats $\Delta h_{1,exp}$ (stage 1, UV at 30 °C), $\Delta h_{2,exp}$ (stage 2, postcuring at 10 K/min after UV stage 1) and $\Delta h_{tot,exp}$ (obtained at 10 K/min). T_g before and after each curing stage (o , int and ∞ indicate before stage 1, after stage 1 and after stage 2, respectively).

Formulation	T_{go} (°C)	T_{gint} (°C)	$T_{g\infty}$ (°C)	$\Delta h_{1,exp}$ (J/g)	$\Delta h_{1,theo}$ (J/g)	$\Delta h_{2,exp}$ (J/g)	$\Delta h_{2,theo}$ (J/g)	$\Delta h_{tot,exp}$ (J/g)	$\Delta h_{tot,theo}$ (J/g)
E100	-75	19	19	273	273	0	0	276	273
E80DGMA20	-69	-3	35	220	219	65	65	286	284
E60DGMA40	-63	-16	51	162	164	130	131	292	295
E40DGMA60	-56	-23	62	107	109	195	196	303	305
E20DGMA80	-49	-31	80	53	55	260	261	313	316
DGMA100	-41	-41	159	0	0	327	327	327	327

Table 2. First-order rate constants and correlation coefficients for the photopolymerization of ExDGMAy at 30 °C

Formulation	k (min ⁻¹)	r
E100	9.1	0.9988
E80DGMA20	6.7	0.9982
E60DGMA40	5.0	0.9983
E40DGMA60	4.0	0.9954
E20DGMA80	2.9	0.9938

Table 3. Kinetic parameters determined by isoconversional integral of non-isothermal stage 1 curing of E100 (neat thermal stage1)

α	E (kJ/mol)	$\ln \left[\frac{AR}{g(\alpha)E} \right]$ (min)	$\ln A^a$ (min ⁻¹)	$k_{150^\circ C}^a$ (min ⁻¹)	r
0.1	190	48.53	57.29	28.11	0.9933
0.2	195	49.72	59.09	42.48	0.9949
0.3	200	50.93	60.72	54.44	0.9963
0.4	206	52.58	62.73	66.21	0.9975
0.5	215	55.07	65.55	78.42	0.9988
0.6	226	57.74	68.56	84.00	0.9989
0.7	231	58.77	69.94	70.19	0.9980
0.8	223	55.55	67.08	39.94	0.9983
0.9	195	46.19	58.17	15.99	0.9991
Average	210	53.21	63.67	55.40	0.9983

^a Pre-exponential factor and rate constant determined by using the isoconversional parameters and the autocatalytic model (see Table 4)

Table 4. Kinetic parameters determined by model fitting analysis of non-isothermal stage 1 curing of E100 (neat thermal stage1)

n	m	E (kJ/mol)	$\ln A$ (min ⁻¹)	r	$k_{30^\circ C}$ (min ⁻¹)	$k_{150^\circ C}$ (min ⁻¹)
1.73	0.27	207	62.51	0.9939	$2.98 \cdot 10^{-9}$	38.9

Table 5. Kinetic parameters determined by isoconversional integral of non-isothermal stage 1 curing of DGMA100 (neat thermal stage2)

α	E (kJ/mol)	$\ln \left[\frac{AR}{g(\alpha)E} \right]$ (min)	$\ln A^a$ (min ⁻¹)	$k_{150^\circ C}^a$ (min ⁻¹)	r
0.1	74	10.76	19.42	0.18	0.9964
0.2	75	10.57	19.66	0.17	0.9983
0.3	76	10.36	19.73	0.16	0.9989
0.4	76	10.20	19.79	0.15	0.9992
0.5	77	10.05	19.85	0.15	0.9994
0.6	77	9.86	19.87	0.15	0.9995
0.7	76	9.59	19.82	0.16	0.9995
0.8	76	9.19	19.69	0.17	0.9995
0.9	74	8.60	19.49	0.20	0.9991
Average	76	9.92	19.72	0.16	0.9993

^a Pre-exponential factor and rate constant determined by using the isoconversional parameters and the autocatalytic model (see Table 6)

Table 6. Kinetic parameters determined by model fitting analysis of non-isothermal stage 2 curing of DGMA100 (neat thermal stage 2)

n	m	E (kJ/mol)	$\ln A$ (min ⁻¹)	r	$k_{30^\circ C}^a$ (min ⁻¹)	$k_{150^\circ C}^a$ (min ⁻¹) ^b
1.51	0.49	75	19.61	0.9959	$3.38 \cdot 10^{-5}$	0.16

Table 7. Kinetic parameters determined by isoconversional integral non-isothermal curing of E40DGMA60

α	E (kJ/mol)	$\ln \left[\frac{AR}{g(\alpha)E} \right]$ (min)	$\ln A^a$ (min ⁻¹)	$\ln k_{150^\circ\text{C}}^a$ (min ⁻¹)	r
0.1	152	37.9	46.33	1.40	0.9944
0.2	161	35.51	44.53	1.06	0.9975
0.3	149	28.51	37.81	0.45	0.9949
Average 1	153	34.41	43.36	0.99	0.9961
0.5	77	9.64	19.34	0.10	0.9981
0.6	76	8.96	18.87	0.08	0.9978
0.7	74	8.24	18.38	0.08	0.9976
0.8	73	7.55	17.98	0.08	0.9974
0.9	72	6.96	17.83	0.09	0.9972
Average 2	74	8.26	18.46	0.08	0.9993

^a Pre-exponential factor and reaction rate determined by using the isoconversional parameters and the autocatalytic model (see Table 8). $g(\alpha)$ was determined using relative conversion from 0 to 1 for each stage

Table 8. Kinetic parameters determined by model fitting analysis of both stages of E40DGMA60

n	m	E (kJ/mol)	$\ln A$ (min ⁻¹)	r	$k_{30^\circ\text{C}}$ (min ⁻¹)	$k_{150^\circ\text{C}}$ (min ⁻¹)
Stage 1						
1.78	0.22	151	43.93	0.9991	$1.7 \cdot 10^{-7}$	2.59
Stage 2						
1.56	0.44	74	18.38	0.9936	$2.08 \cdot 10^{-5}$	0.081

Table 9. Kinetic parameters of both stages determined by isoconversional integral procedure after deconvolution.

α	E (kJ/mol)		$\ln \left[\frac{AR}{g(\alpha)E} \right]$ (min)		$\ln A^a$ (min ⁻¹)		$k_{150^\circ C}^a$ (min ⁻¹)	
	1	2	1	2	1	2	1	2
0.1	166	93	39.50	14.84	47.88	23.63	2.23	0.05
0.2	170	85	40.42	12.11	49.47	21.24	3.11	0.05
0.3	177	81	42.14	10.72	51.66	20.09	4.05	0.05
0.4	174	79	41.10	9.76	50.96	19.33	4.15	0.05
0.5	172	73	39.98	8.02	50.14	17.72	3.97	0.05
0.6	168	75	38.69	8.32	49.16	18.27	3.67	0.05
0.7	161	73	36.11	7.63	46.88	17.78	3.13	0.06
0.8	152	71	33.08	6.99	44.23	17.41	2.60	0.06
0.9	145	65	30.26	5.22	42.00	15.99	2.17	0.08
Average	166	77	39.78	8.32	48.36	19.01	3.30	0.056

^a Pre-exponential factor and rate constant determined by using the isoconversional parameters and the autocatalytic model (see Table 10)

Table 10. Kinetic parameters determined by model fitting analysis of both stages of E40DGMA60 by deconvolution

n	m	E (kJ/mol)	$\ln A$ (min ⁻¹)	r	$k_{30^{\circ}\text{C}}$ (min ⁻¹)	$k_{150^{\circ}\text{C}}$ (min ⁻¹)
Stage 1						
1.79	0.21	164	47.78	0.9999	$2.91 \cdot 10^{-8}$	3.07
Stage 2						
1.53	0.47	74	18.87	0.9944	$9.44 \cdot 10^{-6}$	0.05

Table 11. Kinetic parameters determined by isoconversional integral of non-isothermal stage 2 curing of E40DGMA60 (neat stage2 after stage 1 UV)

α	E (kJ/mol)	$\ln \left[\frac{AR}{g(\alpha)E} \right]$ (min)	$\ln A^a$ (min ⁻¹)	$k_{150^{\circ}\text{C}}^a$ (min ⁻¹)	r
0.1	72	9.28	17.88	0.07	0.9988
0.2	74	9.24	18.28	0.07	0.9998
0.3	74	9.05	18.38	0.06	0.9999
0.4	75	8.89	18.44	0.06	1.0000
0.5	74	8.62	18.38	0.06	1.0000
0.6	74	8.23	18.19	0.06	0.9999
0.7	73	7.81	17.99	0.07	0.9999
0.8	73	7.49	17.94	0.07	0.9997
0.9	73	7.35	18.23	0.07	0.9992
Average	74	8.62	18.20	0.066	0.9998

^a Pre-exponential factor and rate constant determined by using the isoconversional parameters and the autocatalytic model (see Table 12)

Table 12. Kinetic parameters determined by model fitting analysis of non-isothermal stage 2 curing of E40DGMA60 (neat stage 2 after stage 1 UV)

n	m	E (kJ/mol)	$\ln A$ (min ⁻¹)	r	$k_{30^\circ\text{C}}$ (min ⁻¹)	$k_{150^\circ\text{C}}$ (min ⁻¹)
1.51	0.49	74	18.17	0.9999	$1.69 \cdot 10^{-5}$	0.066

Table 13. Isokinetic parameters calculated by using Eq. (9) from isoconversional data for $n+m=2$ model.

Formulation	a (mol/kJ)	b (min ⁻¹)	T_{iso} (°C)	k_{iso} (min ⁻¹)	r
E100 (neat stage 1)	0.318	-3.467	103	0.0312	0.9978
E40DGMA60 (dual stage 1)	0.305	-2.219	121	0.1087	0.9984
DGMA100 (neat stage 2)	0.273	-0.866	167	0.4208	0.9985
E40DGMA60 (dual stage 2)	0.245	0.172	218	1.1876	0.9956